

BULETINUL INSTITUTULUI POLITEHNIC DIN IAȘI  
Publicat de  
Universitatea Tehnică „Gheorghe Asachi” din Iași  
Volumul 64 (68), Numărul 4, 2018  
Secția  
ELECTROTEHNICĂ. ENERGETICĂ. ELECTRONICĂ

## USE OF NUMERICAL METHODS IN STUDY OF TRANSIENT PROCESSES OF DIRECT-ON-LINE CONNECTING OF LOW POWER ASYNCHRONOUS MOTORS

BY

ION VLAD\*, AUREL CÂMPEANU, SORIN ENACHE and  
MONICA ENACHE

University of Craiova,  
Faculty of Electrical Engineering

Received: September 11, 2018

Accepted for publication: October 15, 2018

**Abstract.** The opportunity of the research is explained by the fact that in the present economical and technical circumstances, an interrelation between the optimal design of asynchronous motor, afferent to the steady state and dynamic behaviour is necessary. Knowing the dynamic behaviour of asynchronous motor is the premise of carrying out some high-performance electrical drives. In case of low power asynchronous motors, highly stressed electrically and magnetically, it is imposed to pre-establish, qualitatively and quantitatively, the dynamic processes afferent to the use domain, fact that produced major investments in extensive research in great laboratories. The analysis carried out with an asynchronous motor rated at  $P = 1.0$  kW, considering variable parameters, led to the following results: starting current  $I_p = 7.98 \times I_N$ , starting time  $t_p = 0.17$ s.

**Keywords:** low power; asynchronous motors; transient states; simulation.

### 1. Introduction

Owing to the direct and indirect interaction of people with low power asynchronous motors used in the operation of medical equipments, industrial

---

\*Corresponding author: *e-mail*: ivlad@em.ucv.ro

robots, household uses, these must satisfy the highest standards of safety, reliability and precision.

For instance, in case of medical equipments or robots, the driving asynchronous motor is a precision component and not an auxiliary one (Brunner, 2007; Centner *et al.*, 2008). In such circumstances, the asynchronous motor is mechanically and electrically stressed and, for an adequate operation, it is necessary to know the quantities specific to the state.

## 2. Mathematical Model of Asynchronous Motor

Using some precise mathematical models imposes to consider the influence of the magnetic saturation and of the current pressing upon the machine parameters. Thus, a non-linear system of differential equations results, that can only be solved by means of the computer (Boukhelifa *et al.*, 2004).

The mathematical model used contains the two-axis theory equations, with rotor quantities related to the stator, written in a reference frame fix relatively the stator ( $\omega_B = 0$ ),

$$\begin{aligned}
 \frac{di_{ds}}{dt} &= \frac{1}{L_s L_r' - L_{sh}^2} \left[ -R_s L_r' i_{ds} + \omega L_{sh}^2 i_{qs} + \right. \\
 &\quad \left. + R_r' L_{sh} i_{dr}' + \omega L_r' L_{sh} i_{qr}' + L_r' u_{ds} + 0 \right], \\
 \frac{di_{qs}}{dt} &= \frac{1}{L_s L_r' - L_{sh}^2} \cdot \left[ -\omega L_{sh}^2 i_{ds} - R_s L_r' i_{qs} - \right. \\
 &\quad \left. - \omega L_r' L_{sh} i_{dr}' + R_r' L_{sh} i_{qr}' + 0 + L_r' u_{qs} + 0 \right], \\
 \frac{di_{dr}'}{dt} &= \frac{1}{L_s L_r' - L_{sh}^2} \left[ R_s L_{sh} i_{ds} - \omega L_s L_{sh} i_{qs} - \right. \\
 &\quad \left. - R_r' L_s i_{dr}' - \omega L_s L_r' i_{qr}' - L_{sh} u_{ds} + 0 \right], \\
 \frac{di_{qr}'}{dt} &= \frac{1}{L_s L_r' - L_{sh}^2} \left[ \omega L_s L_{sh} i_{ds} + R_s L_{sh} i_{qs} + \right. \\
 &\quad \left. + \omega L_s L_r' i_{dr}' - R_r' L_s i_{qr}' + 0 - L_{sh} u_{qs} \right].
 \end{aligned} \tag{1}$$

The motion equation is attached to them:

$$\frac{d\omega}{dt} = \frac{p}{J} \left[ \frac{3}{2} p L_{sh} (i_{qs} i_{dr}' - i_{ds} i_{qr}') - m_r \right], \tag{2}$$

where, the square bracket is the electromagnetic torque:

$$m = \frac{3}{2} p L_{sh} (i_{qs} i_{dr}' - i_{ds} i_{qr}'). \tag{3}$$

### 3. Results Obtained by Simulation

The theoretical researches and the experimental tests have been carried out with a squirrel cage asynchronous motor rated as follows:  $P_N = 1.0$  kW – rated power;  $U_N = 400$  V – rated voltage;  $I_{1N} = 2.517$  A – rated current;  $n_1 = 1,500$  r.p.m. – synchronism speed;  $M_N = 6.908$  Nm – rated torque  $s_N = 7.8\%$  – rated slip and parameters  $R_s = 5.366$   $\Omega$ ,  $R'_r = 6.836$   $\Omega$ ,  $L_{s\sigma} = 0.028$  H,  $L'_{r\sigma} = 0.018$  H,  $L_{sh} = 0.412$  H,  $J = 0.011$  kgm<sup>2</sup>. The operation and starting characteristics are:  $\cos\varphi = 0.772$ ;  $\eta = 0.784$ ;  $M_{\max} = 3.38 \times M_N$ ;  $M_p = 2.93 \times M_N$ ;  $I_p = 4.304 \times I_N$ .

#### 3.1. Dynamic State of Asynchronous Motor Starting

The simulations carried out and presented below (Enache *et al.*, 2008; Curteanu, 2004; Tudorache *et al.*, 2009; Vlad *et al.*, 2017) take into consideration the no-load starting of low power asynchronous motor ( $M_{st} = 0.1 \times M_N = 0.693$  Nm) in two situations:  $J_2 = 1 \times J = 0.011$  kgm<sup>2</sup> – the inertia moment is that of the motor;  $J_2 = 80 \times J = 0.179$  kgm<sup>2</sup> – the mechanism coupled has a very high inertia moment and negligible resistant torque.

The electromechanical transient process generates high oscillations in the curve of the electromagnetic torque (Câmpeanu *et al.*, 2012; Kovacs, 1980); the longer the starting time is, the more and higher the oscillations are.

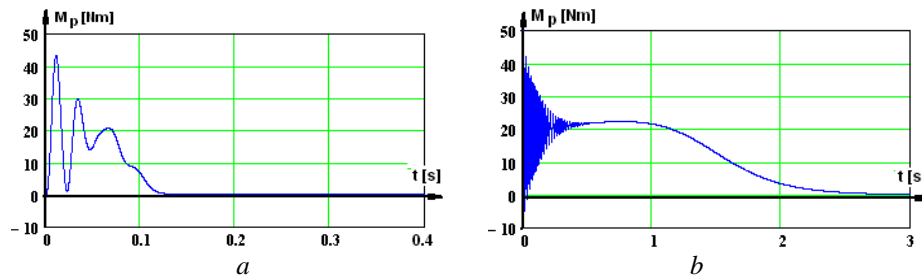


Fig. 1 – Variation curves for the electromagnetic torque in case of no-load starting:  
a – for  $J_2 = 0.011$  kgm<sup>2</sup>; b –  $J_2 = 0.179$  kgm<sup>2</sup>.

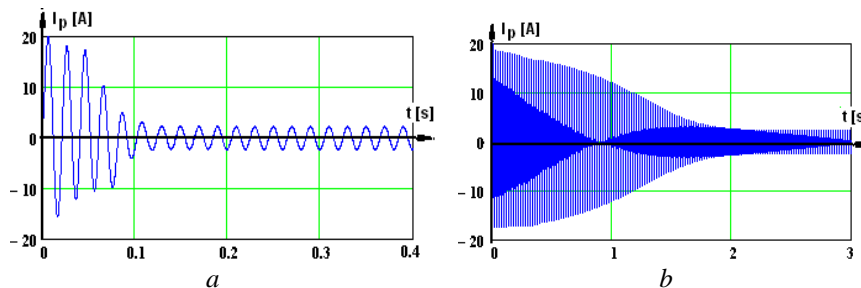


Fig. 2 – Variation curves for the stator current in case of no-load starting:  
a – for  $J_2 = 0.011$  kgm<sup>2</sup>; b –  $J_2 = 0.179$  kgm<sup>2</sup>.

In our case, the analysis carried out considers a low power asynchronous motor. Consequently, the simulations presented in Fig. 1 emphasize few low oscillations in the curve of the electromagnetic torque. The momentary torques, in case of no-load starting of the motor are depicted in Fig. 1 *a*; these torques are very few, but have high values. The motor coupling to the mechanism that has a high inertia moment, Fig. 1 *b*, and direct-on-line connecting of the motor show that we have many torque oscillations and the starting time increases a lot. The same explanations are also for the curves of the currents, presented in Fig. 2. High inertia moments make to appear very few oscillations in the speed curves (Fig. 3 *a*), respectively no oscillations (Fig. 3 *b*).

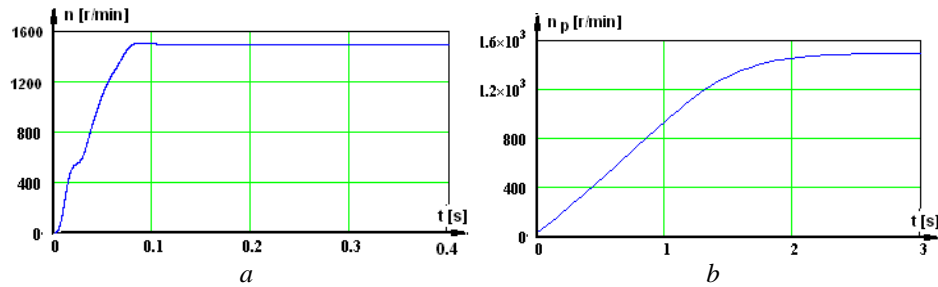


Fig. 3 – Variation curves of the speed in case of no-load starting:  
*a* – for  $J_2 = 0.011 \text{ kgm}^2$ ; *b* –  $J_2 = 0.179 \text{ kgm}^2$ .

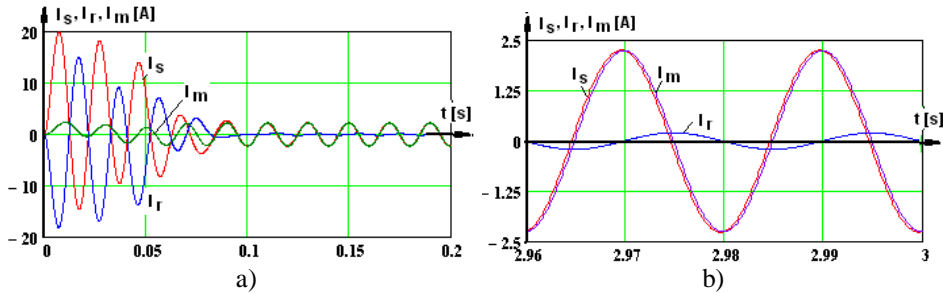


Fig. 4 – Variation curves of the phase currents:  $I_s$  – stator,  $I_r$  – rotor,  $I_m$  – magnetization:  
*a* – during the starting; *b* – in stabilized state.

Because the load torque is very low, in stable operation state, Fig. 4, we notice a very low rotor phase current, almost equal stator and magnetization phase currents, fact known from the design. In the first moments of the direct-on-line connecting (no load), we see very high stator and rotor phase currents, almost equal and in opposition, which are damped fast, Fig. 4 *a*, and the magnetization current has a light transient state. The simulations carried out for a high inertia moment allow us to compute, on each voltage period, the average or root-mean-square values, in order to determine the torque characteristic, Fig. 5 *a*, the current characteristic, Fig. 5 *b*, the speed characteristic, Fig. 5 *c*, respectively the power factor characteristic, Fig. 5 *d*. Analyzing the torque curve,

Fig. 5 *a*, we see that at starting  $M_p = 20.85 \text{ Nm} = 3.018 \times M_N$ , then immediately after starting, a minimum value occurs  $M_{\min} = 19.278 \text{ Nm} = 2.797 \times M_N$ ; after that, the torque increases to the maximum value  $M_m = 23.374 \text{ Nm} = 3.374 \times M_N$ , and finally it is stabilized at the resistant torque value,  $M_m = M_{st} = 0.69 \text{ Nm}$ .

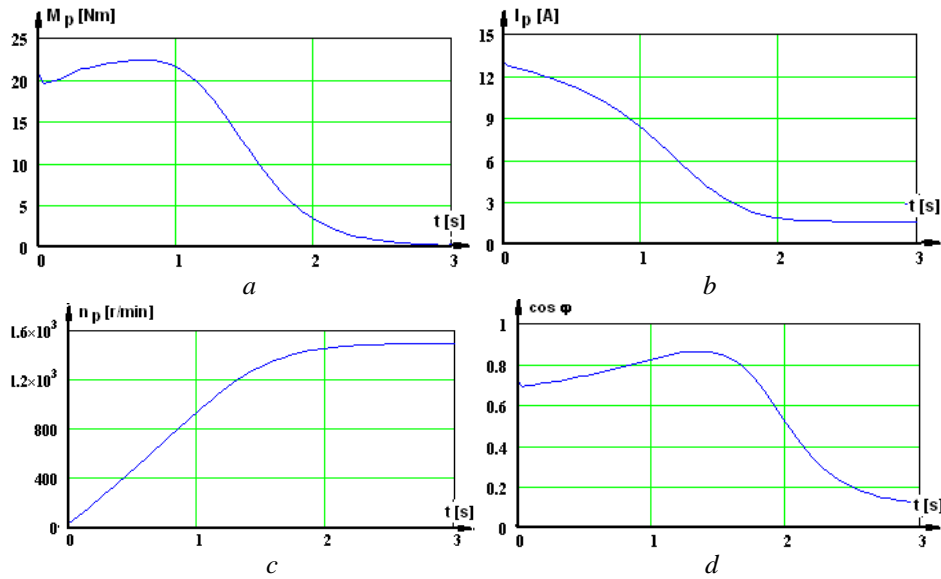


Fig. 5. Variation curves during the starting: *a* – the average value of the torque; *b* – the root-mean-square value of the current; *c* – the average value of the speed.

Using the curves depicted in Fig. 5, by removing the variable  $t$  – time, the natural mechanical characteristic is obtained,  $m_p=f(s)$ , which is plotted in per unit in Fig. 6 *a*. The same characteristic, Fig. 6 *b*, can be determined in the design stage. Similarly, the curves of the currents, during the starting, are presented in Fig. 7, simulated by means of the mathematical model proposed, respectively obtained by design.

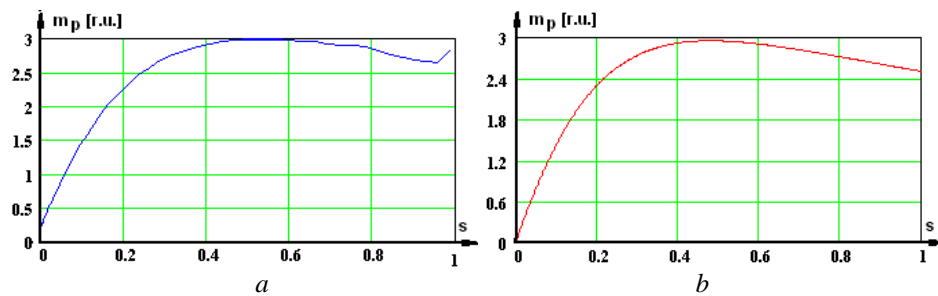


Fig. 6 – Natural mechanical characteristics: *a* – determined by simulation in dynamic state; *b* – determined by design.

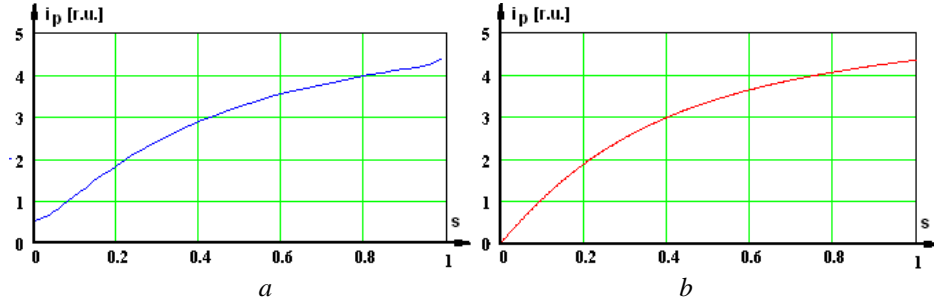


Fig. 7 – Current characteristics in quasi-steady state: *a* – determined by simulation in dynamic state; *b* – classically determined classically, by design.

Analyzing the curves from Figs. 6 and 7, we notice that they are almost identical, fact that confirms the correctness of the simulations presented.

### 3.2. Experimental Results

The experimental tests for direct-on-line connecting of the asynchronous motor have been carried out by using the scheme presented in Fig. 8, where the notations used are:

– M.A. three-phase squirrel cage asynchronous motor, rated as follows:  
 $P_N = 1.0 \text{ kW}$ ,  $U_N = 380 \text{ V}$ ,  $I_N = 2.517 \text{ A}$ ,  $n_1 = 1,500 \text{ r.p.m.}$

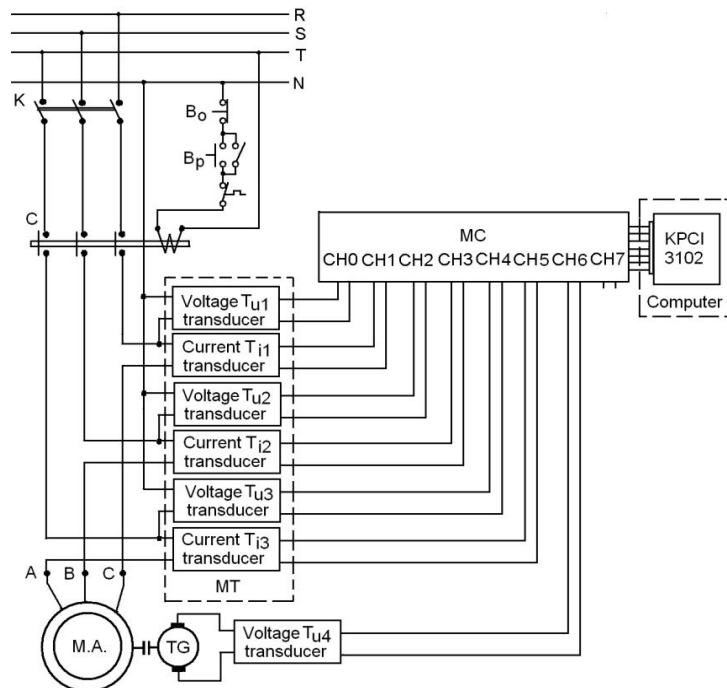


Fig. 8 – Experimental assembly.

– KPCI 3102 acquisition board with high-speed analogical and digital interfaces, assembled inside the computer (KPCI-3104A.pdf).

As we can notice in Fig. 8, in order to acquire the seven signals we want (currents and voltages of the three phases and the speed) current and voltage transducers have been used.

– MT module with current and voltage transducers is used for adapting the currents and the voltages measured to the values required by the acquisition system;

– MC connections module makes the convenient connection of the signal sources to the data acquisition board.

By means of the module, all the channels of the acquisition board are connected to the labelled terminals, where the banana-conductors are connected, making link with the signal sources.

– TG permanent-magnet direct current tachogenerator that provides a voltage proportional with the machine speed (100 V at 1500 r.p.m).

–  $B_p$  button for direct-on-line connecting of the asynchronous motor;

–  $B_o$  button for disconnecting from the network.

There are presented forwards the results of the experimental tests carried out with the scheme depicted in Fig. 8, for the dynamic starting state by direct-on-line connecting to the network, the stabilized state and, respectively for disconnecting.

In Fig. 9 there are presented curves for current, during the no-load starting, simulated curves and experimentally established curves.

The comparison between the curves obtained by modelling (simulation) and the curves obtained experimentally Fig. 9 shows that insignificant differences occur, justified by the fact that the machine inductances have been considered variable – dependent upon the saturation with the motor load and the losses torque at no-load starting  $M_{st} = \text{constant}$ .

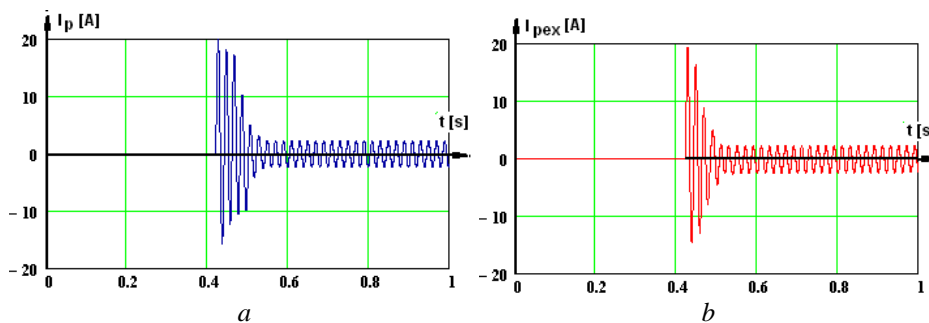


Fig. 9 – Phase currents curves during the starting period: *a* – curves established by simulation *b* – curve experimentally established.

For the starting we analyzed, the experimental results shows a no-load current  $I_{10} = 1.599$  A, the shock current  $I_{1\max} = 20.1$  A or, in per unit  $i_{1\max0} = I_{1\max}/I_{10} = 20.1/1.599 = 12.51$ , respectively,  $i_{1\maxN} = I_{1\max}/I_{1N} = 20.1/2.517 = 7.98$ .

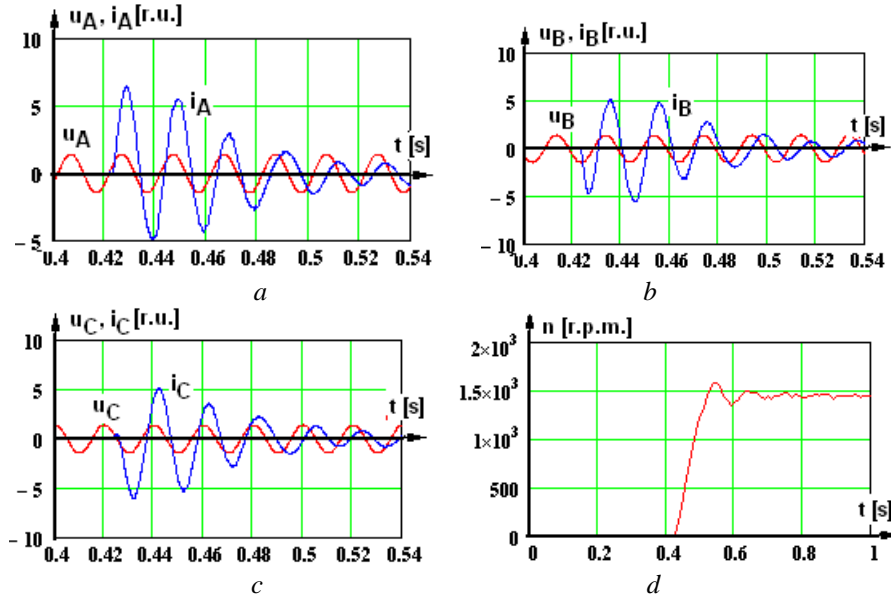


Fig. 10 – Curves of voltages and currents during the transient starting state of the asynchronous motor, by direct-on-line connecting to the network:  
*a* – phase A; *b* – phase B; *c* – phase C; *d* – speed curve.

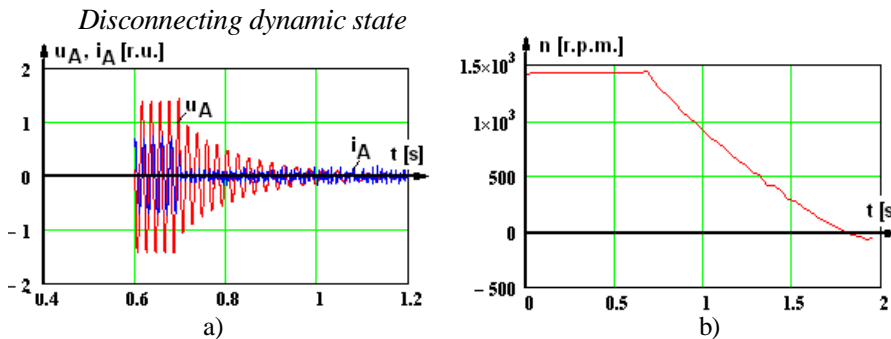


Fig. 11 – Dynamic state for motor disconnecting from the network:  
*a* – current and voltage curves, phase A; *b* – speed curve.

In steady state we only find the input active power necessary for the motor losses:  $P_1 = 219 \text{ W}$ ,  $S_1 = 1,063 \text{ VA}$ ,  $Q_1 = 1,042 \text{ VAR}$ ,  $I_{10} = 1.613 \text{ A}$ ,  $\cos \varphi_{10} = 0.196$ ,  $P_2 = 0.002 \text{ W}$ ,  $M = 0.70 \text{ Nm}$ ,  $n_{10} = 1,491 \text{ r.p.m.}$ ,  $s = 0.0007$ ,  $\Sigma p = 113.1 \text{ W}$ ,  $p_{\text{mec}} = 22 \text{ W}$ ,  $p_{\text{Cu1}} = 38 \text{ W}$ ,  $p_{\text{Cu2}} = 0.000015 \text{ W}$ , values which are also found experimentally, Fig. 12 *b*. Experimentally, by using the data acquisition system, there have been established the variation curves of the stator voltages and currents, on each phase, during the starting period (in per unit), Fig. 10 *a*, 10 *b*, 10 *c* and the speed curve, Fig. 10 *d*. If we analyze these figures, we can establish the connecting moment for each phase. A data acquisition has been

made for the motor disconnecting, Fig. 11, where we notice a residual value of the current and a decrease of the induced electromotive force, because the magnetic field does not extinguish suddenly. The variation curve of the speed, Fig. 11 *b* and the motion equation allow us to establish the losses torque and to notice that it is almost constant (it does not depend upon the speed).

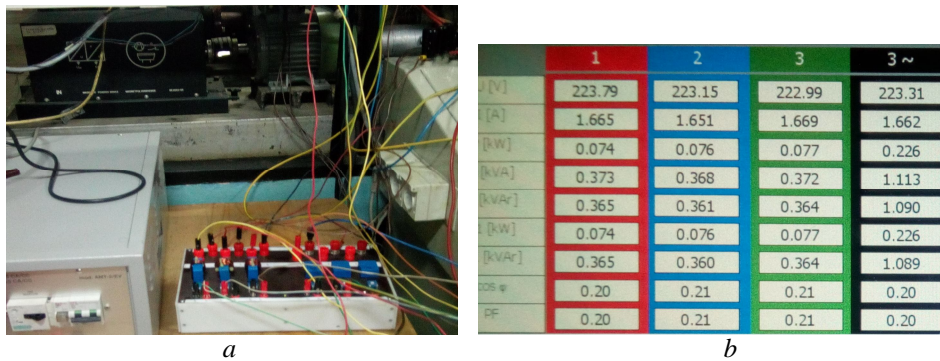


Fig. 12 – Experimental determinations: *a* – scheme of the circuit, module with transducers and the data acquisition system; *b*) experimental data.

#### 4. Conclusions

Using the simulations presented in the paper, the characteristics of the torque and current can be determined in case of direct-on-line starting of the asynchronous motor analyzed. The starting current is determined by simulation and experimentally and it is noticed that the error which occurs is low,  $\Delta I_p < < 1.6\%$ . The starting time was 0.17 s and the speed has low damped oscillations.

**Acknowledgments.** This paper was realized under the frame of the grant POC 59/05.09.2016, ID: P\_40\_401, SMIS 106021.

#### APPENDIX

$i_{ds}, i_{qs}$  – stator currents by the  $d$  and  $q$  axes;  
 $i'_{dr}, i'_{qr}$  – related rotor currents by the  $d$  and  $q$  axes;  
 $u_{ds}, u_{qs}$  – stator voltages by the  $d$  and  $q$  axes;  
 $L_{ss}, L'_r, L_{sh}$  – stator/rotor leakage inductances, respectively main inductance;  
 $R_s, R'_r$  – stator/rotor phase resistances;  
 $p$  – number of pole pairs;  
 $\omega$  – angular rotor speed;  
 $m, m_r$  – the electromagnetic and load torques,  
 $J$  – the rotor inertia.

## REFERENCES

- Boukhelifa A., Kherbouch M., Cheriti A., Ibtouen R., Touhami O., Tahmi R, *Stator Current Minimization by Field Optimization in Induction Machine*, Internat. Conf. on Electrical, Electronic and Computer Engineering, ICEEC'04, 2004.
- Brunner C.U., *International Standards for Electric Motors*, Standards for Efficiency of Electric Motor Systems (SEEEM), 2007, 6-10.
- Campeanu A., Vlad I., Enache S., Augustinov L., Liuba G., Cautil I., *Optimization of Startup Characteristics of Medium Power Asynchronous Motors with Short Circuit Rotor*, ICEM'2012, Marseille, France.
- Centner M., Schäfer U., *Machine Design Software for Induction Machines*, in Proc. ICEM, Vilamoura, Portugal, 2008, 1-4.
- Curteanu S., *Numerical Computation and Symbols in MATHCAD*, Matrix Rom Publishing House, Bucharest, 2004 (in Romanian).
- Enache S., Câmpeanu A., Vlad I., Enache M., *Determination of Asynchronous Machine Parameters by a Dynamic Test*, 11<sup>th</sup> Internat. Conf. on Optimization of Electrical and Electronic Equipment OPTIM'08, 2008, Brasov, Romania, 57-63.
- Kovacs P., *Analysis of Transient States of Electrical Machines*, Technical Publishing House, Bucharest, 1980 (in Romanian).
- Tudorache T., Melcescu L., *FEM Optimal Design of Energy Efficient Induction Machines*, AECE Journal, **9(2)**, 58-64 (2009).
- Vlad I., Câmpeanu A., Enache S., Enache Monica-Adela, *Dynamic State of Low Power Asynchronous Motors in Direct-on-Line Starting*, Annals of the University of Craiova, Electrical Engineering Series, **41**, 54-59 (2017).
- \* \* <http://www.testequity.com/documents/pdf/keithley/KPCI-3101A-KPCI-3102A-KPCI-3103A-KPCI-3104A.pdf>

UTILIZAREA METODELOR NUMERICE ÎN STUDIUL  
 PROCESELOR TRANZITORII DE CONECTARE LA REȚEA A  
 MOTOARELOR ASINCRONE DE PUTERI MICI

(Rezumat)

Oportunitatea cercetării se explică prin faptul că în contextul actual economic și tehnic este necesară o interferență între proiectarea optimală a motorului asincron, aferentă regimului staționar și comportarea dinamică. Cunoașterea comportării dinamice a motorului asincron reprezintă premiza realizării unor acționări electrice înalt performante. La motoarele asincrone de puteri mici, intens solicitate electric și magnetic, se impune predeterminarea calitativă și cantitativă a proceselor dinamice aferente domeniului de utilizare, fapt ce a determinat investiții majore în cercetări de amploare în marile laboratoare. Analiza făcută pe un motor asincron cu puterea  $P = 1.0$  kW, considerând parametrii variabili, a dus la următoarele rezultate: curent de pornire  $I_p = 7.98 \times I_N$ , durata pornirii  $t_p = 0.17$  s.